

Coamorphous Drug Systems: Enhanced Physical Stability and Dissolution Rate of Indomethacin and Naproxen

Korbinian Löbmann,[†] Riikka Laitinen,[†] Holger Grohgan,[‡] Keith C. Gordon,[§] Clare Strachan,[†] and Thomas Rades^{*,†}

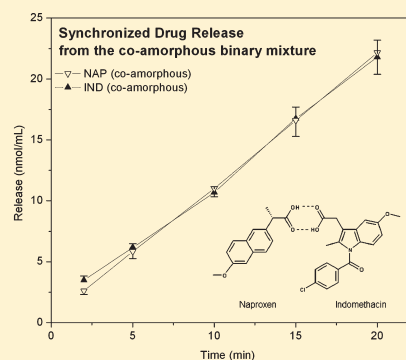
[†]School of Pharmacy, University of Otago, Dunedin, New Zealand

[‡]Department of Pharmaceutics and Analytical Chemistry, The Faculty of Pharmaceutical Sciences, University of Copenhagen, Copenhagen, Denmark

[§]Department of Chemistry and MacDiarmid Institute for Advanced Materials and Nanotechnology, University of Otago, Dunedin, New Zealand

ABSTRACT: One of the challenges in drug development today is that many new drug candidates are poorly water-soluble, and one of the approaches to overcome this problem is to transfer a crystalline drug into its amorphous form, thus increasing dissolution rate and apparent solubility of the compound. In this study, a coamorphous drug/drug combination between the two nonsteroidal anti-inflammatory drugs, naproxen and γ -indomethacin, was prepared and investigated. At molar ratios of 2:1, 1:1 and 1:2, the drugs were quench cooled in order to obtain a coamorphous binary phase. Physical stability was examined at 277.15 and 298.15 K under dry conditions (phosphorus pentoxide) and analyzed with X-ray powder diffraction (XRPD). Intrinsic dissolution testing was carried out to identify dissolution advantages of the coamorphous form over its crystalline counterparts or amorphous indomethacin. Fourier transform infrared spectroscopy (FTIR) was used for analyses at the molecular level to detect potential molecular interactions. Differential scanning calorimetry (DSC) thermograms were employed to assess the glass transition temperatures (T_g), and the results were compared with predicted T_g s from the Gordon–Taylor equation. Results showed that naproxen could be made amorphous in combination with indomethacin while this was not possible with naproxen alone. Peak shifts in the FTIR spectra indicated molecular interactions between both drugs, and it is suggested that the two drugs formed a heterodimer. Therefore, samples at the 1:2 and 2:1 ratios showed recrystallization of the excess drug upon storage whereas the 1:1 ratio samples remained amorphous. Intrinsic dissolution testing showed increased dissolution rate of both drugs in the coamorphous form as well as a synchronized release for the 1:1 coamorphous blend. All T_g s displayed negative deviations from the Gordon–Taylor equation with the 1:1 ratio showing the largest deviation. In a novel approach of predicting the glass transition temperature, the 1:1 drug ratio was inserted as an individual component in the Gordon–Taylor equation with the excess drug representing the second compound. This approach resulted in a good fit to the experimentally determined T_g s.

KEYWORDS: coamorphous, naproxen–indomethacin, synchronized release, intrinsic dissolution, Gordon–Taylor equation, stability



1. INTRODUCTION

A major challenge in drug development today is that many new drug candidates are poorly water-soluble.¹ One of the approaches to overcome this problem is to transfer a crystalline drug into an amorphous form, thus increasing dissolution rate and apparent solubility of the compound.^{1,2} The main drawback of using amorphous drugs in dosage forms is the limited and largely unpredictable physical stability of amorphous forms during manufacturing or storage, due to crystallization of this thermodynamically unstable state.² Another problem of some amorphous systems is solvent-induced crystallization upon oral application.^{1,3} Thus, the solubility and dissolution rate advantage might be lost in spite of stability under dry conditions. It is therefore necessary to find ways to stabilize an amorphous drug system upon storage and after administration.

One strategy to improve the physical stability of amorphous drugs and their dissolution behavior is to incorporate them into amorphous polymers in order to create a (single phase) glass solution.⁴ The increased physical stability of these amorphous systems can be explained by the increased glass transition temperature (T_g) of the glass solution, compared to the neat amorphous drug, resulting from the usually high T_g of polymers.⁵ Moreover, some polymers contain functional groups, such as the carbonyl group of the lactam ring in polyvinylpyrrolidone (PVP), which can act as proton acceptors and allow for intermolecular H-bondings between drug and polymer. In such cases, molecular

Received: June 13, 2011

Accepted: August 4, 2011

Revised: July 26, 2011

Published: August 04, 2011

interactions can further stabilize the amorphous state of the solid dispersion, by lowering the molecular mobility of the drug, and thus their ability to nucleate and crystallize.⁶ However, the majority of polymers used in the formulation of glass solutions absorb moisture, which acts as a potent plasticizer for the amorphous system, strongly reducing its T_g while increasing molecular mobility. This may facilitate phase separation and crystallization.⁷ Furthermore, due to the limited solubility of some drugs in the polymeric carrier, large quantities of polymer might be required for incorporating a therapeutic drug dose into the glass solution, leading to high polymer:drug ratios and thus prohibitively large bulk volumes of the final dosage form.⁸ Other drawbacks of drug–polymer glass solutions include drug–carrier incompatibility, difficulties in pulverization, poor flow properties and compressibility, due to the sometimes soft and tacky nature of the materials, as well as sticking of the dispersion system to dies and punches.^{8–10} Thus, there is a clear need for additional or alternative ways to stabilize amorphous drugs.

Coamorphous binary combinations of two drugs or a drug and a small molecule excipient might prove to be an interesting alternative to drug–polymer combinations. This approach can also create solubility advantages and stabilize the amorphous system, e.g. through intermolecular interactions, and might overcome limitations associated with solid dispersions. Chieng et al. discovered in 2009 that a mixture of the two drugs indomethacin and ranitidine prepared by vibrational ball milling led to a highly stable amorphous binary mixture.¹¹ Allesø et al. (2009) showed that an amorphous mixture of cimetidine and naproxen enhanced the dissolution rate of both drugs compared to their crystalline counterparts.¹² Furthermore, preparation of the coamorphous combination in this study resulted in a synchronized drug release, indicating that the drugs may be released as a pair in a 1:1 molar ratio. In another binary mixture study by Yamamura et al. (2000 and 2002), cimetidine in combination with indomethacin¹³ or diflunisal¹⁴ was shown to result in the formation of an amorphous salt by solvent evaporation or precipitation.

In the current study, we investigate a coamorphous drug/drug combination between indomethacin and naproxen. The choice to combine these two drugs was based on two reasons. First, both drugs are nonsteroidal anti-inflammatory drugs and in this regard are pharmacologically complementary in their use in pain relief. Second, being class 2 drugs in the biopharmaceutics classification system (BCS), transforming both drugs into their amorphous, and thus more soluble, forms would be desirable in enhancing their bioavailability.

In this study, coamorphous mixtures of naproxen and indomethacin in varying molar ratios were produced via quench cooling from the melt and characterized with respect to their thermal and structural properties, molecular interactions, physical stability, and intrinsic dissolution properties.

2. MATERIALS AND METHODS

2.1. Materials. Naproxen (NAP, $M = 230.26$ g/mol) and indomethacin (IND, γ polymorph; $M = 357.79$ g/mol) were sourced from Divis Laboratories, Ltd. USA and Sigma-Aldrich, USA, respectively. Both drugs were used as received.

2.2. Methods. *2.2.1. Preparation of the Amorphous Materials.* Coamorphous systems of indomethacin and naproxen were prepared by quench cooling. Quench cooling was selected as preparation method for the coamorphous binary drug mixture as

other attempts, such as vibrational ball milling, cryo ball milling, spray-drying and freeze-drying, did not result in a complete amorphization (data not shown).

A total of 1000 mg in molar ratios of 1:1 (608.1 mg of IND and 391.6 mg of NAP), 1:2 (562.8 mg of IND and 437.2 mg of NAP) and 2:1 (756.6 mg of IND and 243.4 mg of NAP) were prepared as homogeneous physical mixtures prior to quench cooling by gentle mixing in a mortar and pestle for 60 s. These mixtures were then transferred into aluminum dishes and melted in a preheated oven at 441.15 K for 5 min. To obtain the amorphous mixtures, liquid nitrogen was poured onto the samples. The same procedure was conducted for pure IND. The temperature of 441.15 K was chosen as it is above the melting temperature (T_m) of IND, which has a higher melting temperature than NAP ($T_{mIND} = 435.15$ K; $T_{mNAP} = 431.25$ K). The cold sample dishes were then immediately stored in a desiccator over phosphorus pentoxide to avoid moisture sorption until the samples reached room temperature. Then the samples were gently milled with mortar and pestle and further analyzed. The stability of pure NAP in the amorphous form was found to be very low. The drug started to recrystallize immediately when prepared as stated above, making it impossible to further analyze the amorphous form of neat NAP or to obtain its T_g . Thus, amorphous NAP was prepared *in situ* using differential scanning calorimetry (DSC; see section 2.2.2.2.) In order to have comparable results for the glass transition temperatures, pure IND and the three physical mixtures were additionally treated in the same manner.

2.2.2. Analytical Techniques. *2.2.2.1. X-ray Powder Diffraction.* XRPD analysis was performed using an X'Pert PRO X-ray diffractometer (PANalytical, Almelo, The Netherlands; MPD PW3040/60 XRD; Cu K α anode; $\lambda = 1.541$ Å; 40 kV; 30 mA). Samples were filled into an aluminum sample holder and gently compressed by a spatula in order to obtain a compact sample with a smooth surface. For the scans a start angle of $5^\circ 2\theta$ and an end angle of $35^\circ 2\theta$ with a scan speed of $0.1285^\circ 2\theta/\text{min}$ and a step size of $0.0084^\circ 2\theta$ were used.

2.2.2.2. Differential Scanning Calorimetry. DSC thermograms were obtained using a TA-DSC Q100 (V8.2 Build 268, TA-Instruments-Waters LLC, New Castle, DE, USA) under a nitrogen gas flow of 50 mL/min. Calibration for temperature and enthalpy was carried out using indium as a standard. Approximately 7 mg of sample was crimped in an aluminum pan and then analyzed. For the determination of the phase diagram, sample mixtures were heated from 298.15 to 453.15 K. For the measurement of T_g s, samples were melted in the DSC and held isothermally at 441.15 K for 5 min; the sample pan was then immersed in liquid nitrogen while the DSC was cooled to 273.15 K. The sample was then brought to 223.15 K in the DSC and heated to 453.15 K at a heating rate of 10 K min^{-1} . The resulting T_g was calculated as the mean value of a minimum of three independent preparations. Both T_g and T_m were determined using TA-Universal Analysis 2000 software (version 4.7A).

2.2.2.3. Attenuated Total Reflectance FT-Infrared Spectroscopy (ATR-FTIR). Samples were analyzed using a Varian 3100 FTIR (Excalibur series) attached with an attenuated total reflectance accessory (GladiATR, PikeTech, WI, USA). Spectra (64 scans at 4 cm^{-1} resolution) were recorded over a range of $4000\text{--}400\text{ cm}^{-1}$. The ATR diamond crystal and the surrounding stainless steel plate of the ATR device were cooled down with ice prior to the measurements of the samples. This was conducted to ensure measurement conditions below the T_g of NAP (478.19 K) in order to obtain a spectrum of the physically

unstable amorphous NAP. Data was analyzed using Varian Resolution Pro, v4.1.0.101 software and plotted using Origin (version 7.5, OriginLab Corporation, Northampton, MA, USA).

2.2.3. Stability Studies. In the stability study, the coamorphous binary mixtures (2:1, 1:1 and 1:2 molar ratios) were stored in desiccators under dry conditions (phosphorus pentoxide) at 277.15 and 298.15 K for 21 days and repeatedly analyzed by XRPD (at days 0, 7, 14 and 21).

2.2.4. Intrinsic Dissolution Testing. **2.2.4.1. Dissolution Procedure.** For the intrinsic dissolution rate (IDR) studies, powder compacts were compressed with a hydraulic press (Fred S. Carver, Laboratory Press model 3392, Menomonee Falls, WI, USA). Crystalline IND, amorphous IND, crystalline NAP and quench cooled 1:1 IND–NAP mixtures (all 250 mg in total) were compressed at a pressure of 147.5 MPa for 10 s. The compression of the coamorphous 1:1 mixture at room temperature resulted in a glassy disk, where the powder sintered to form a smooth surface. To avoid this (and thus ensure the mixture compacts were similar in surface structure to the single component tablets), the 1:1 mixtures were compressed at 277.15 K. The resulting discs with a surface area of 1.33 cm² were inserted into a PTFE intrinsic dissolution sample holder to achieve a flat surface, consequently only one face of the tablet is exposed to the dissolution medium. The samples were rotated at 50 rpm in 900 mL of 0.1 M phosphate buffer (pH 7.4, 310.15 K) as dissolution medium. 5 mL aliquots were withdrawn (with replacement) at predetermined time points (2, 5, 10, 15, and 20 min) and measured in an Ultrospec 2000 UV–vis spectrophotometer model 80-2106-60 (Pharmacia Biotrech Ltd., Cambridge, U.K.). The analyzing software was SWIFT-wavescan, v1.05 (Pharmacia Biotrech Ltd.), and a spectrum between 220 and 400 nm was recorded. The spectra were then analyzed using a multivariate analysis model to obtain the respective concentrations in mg mL^{−1} for both drugs (see below). Since the surface area of the tablets for the intrinsic dissolution experiment is the same for the pure drugs as for the coamorphous mixtures, the surface areas of the individual components are less when part of a mixture than when compressed alone. Therefore, the release-time profiles were transferred into mg per accessible area (mg cm^{−2}) for each drug. For the samples containing only one drug (crystalline NAP, crystalline IND, and amorphous IND) this was done by dividing the drug release (mg mL^{−1}) by the surface area of the tablet (1.33 cm²) subsequent to multiplying it by 900 mL. In contrast, the release (mg cm^{−2}) for the coamorphous drug mixture was calculated based on an estimation of the accessible surface area for each drug. The powder compacts of 250 mg contain approximately 97.9 mg of NAP and 152.1 mg of IND in the 1:1 molar ratio. With the powder densities of 1.265 g cm^{−3} and 1.379 g cm^{−3} for NAP and IND, respectively, the (theoretical) volume of each drug prior to compression is calculated as 0.0774 cm³ for NAP and 0.1103 cm³ for IND. Assuming a homogeneous mixture in the coamorphous samples the volume will be occupied by 41.2% of NAP and 58.8% of IND. Hence, transferred to the surface area of 1.33 cm², the tablet surface will initially comprise 0.548 cm² of NAP and 0.782 cm² of IND. From these values, the release profiles (mg cm^{−2} versus time) may then be calculated under the assumption that the surface area stays constant throughout the experiment. Dissolution tests were performed in triplicate.

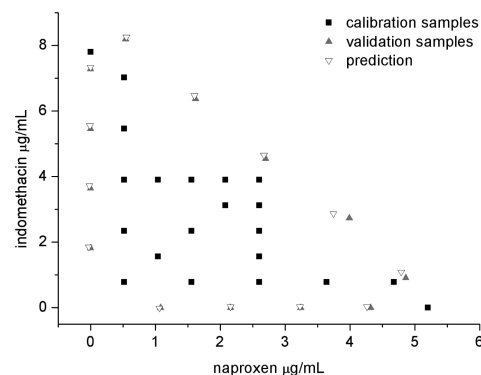


Figure 1. Calibration and validation design with the different concentration of NAP and IND in each sample. Calibration samples are shown as black squares, validation samples are shown as gray triangles, and the predictions of these samples by the partial least-squares regression model are shown as open triangles.

2.2.4.2. UV Calibration Model. A multivariate UV method was used to determine the concentrations of NAP and IND (mg mL^{−1}) in the various samples taken during the dissolution experiment (see above). The method was based on a method previously developed in our group.¹² Briefly, a calibration model with 21 calibration samples of known NAP and IND concentrations was used for prediction, where the UV spectra represent the X matrix and the Y matrix was based on the associated concentration of the drugs. Figure 1 shows the calibration samples with varying concentrations of NAP and IND prepared from stock solutions (NAP: 5.2 µg/mL; IND 7.8 µg/mL) using 0.1 M phosphate buffer (pH 7.4) as dissolution medium. The spectral range was recorded from 220 to 400 nm. In order to extract spectral information relevant to the Y matrix, a nonlinear iterative partial least-squares algorithm (NIPALS) was applied to the recorded UV spectra (i.e., to the X matrix). Spectra were used without preprocessing, and leave-one-out cross validation was used as internal validation. The explained total variance was 99.97845 (X matrix) and 99.97983 (Y matrix) for two factors in the NIPALS model. An external validation with 13 samples of known concentrations of both drugs was performed to further test the model (Figure 1). The obtained root-mean-square values of prediction (RMSEP) for the external validation were 0.088 µg mL^{−1} and 0.101 µg mL^{−1} for NAP and IND, respectively (R² values of observed vs predicted were 0.997 and 0.999). The prediction of NAP at high concentrations showed a slight offset from the true values, and thus samples were diluted to NAP concentrations below 3 µg/mL. Multivariate modeling was performed using *The Unscrambler X* (CAMO Software AS, Oslo, Norway, version 10.0.1).

2.2.5. Theoretical T_g Values (Gordon–Taylor Equation). The experimental glass transition values of the various quench cooled mixtures were compared with the predicted T_g values calculated from the Gordon–Taylor equation:

$$T_{g12} = \frac{w_1 \cdot T_{g1} + K \cdot w_2 \cdot T_{g2}}{w_1 + K \cdot w_2} \quad (1)$$

where T_{g12} is the glass transition temperature (in K) of the coamorphous mixture, whereas T_{g1} and T_{g2} are the glass transition temperatures (in K) of the single amorphous compounds 1 and 2, respectively. The weight fractions of each substance in the

mixture are represented by w_1 and w_2 . K is a constant and can be further described by eq 2:

$$K = \frac{T_{g1} \cdot \rho_1}{T_{g2} \cdot \rho_2} \quad (2)$$

where ρ_1 and ρ_2 are the respective powder densities of the single amorphous components. The densities of 1.265 g/cm^{−3} (± 0.003), 1.379 g/cm^{−3} (± 0.003), 1.334 g/cm^{−3} (± 0.018) and 1.277 g/cm^{−3} (± 0.012) for crystalline NAP, γ -IND, amorphous IND and the coamorphous 1:1 molar ratio between both drugs, respectively, were determined in triplicate using a helium pycnometer (AccuPyc 1330 V3.03, Micrometrics, GA, USA).

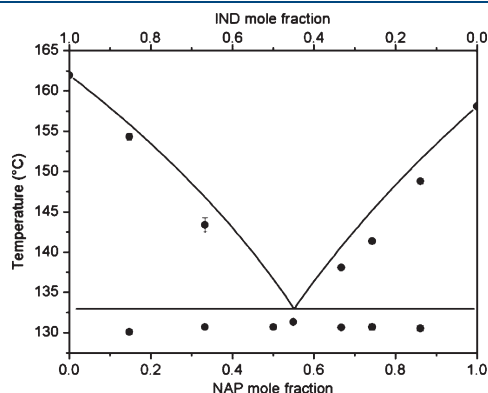


Figure 2. Phase diagram of the NAP– γ -IND binary systems. The black dots represent the experimental melting points and the solid lines represent the theoretical values calculated from the simplified form of the Schröder–Van Laar equation for NAP and γ -IND.

Since the density for amorphous NAP could not be determined due to the fast recrystallization of this drug, the density for crystalline NAP obtained from the helium pycnometer measurements was taken as the value for the amorphous component. This approximation for the amorphous density is valid for small molecules such as NAP.¹² The experimental T_g values for quench cooled NAP, IND and the coamorphous sample at the 1:1 molar ratio (278.19 K, 317.88 K and 298.45 K, respectively) were used for prediction.

2.2.6. Calculation of Melting Point Depression (Schröder–Van Laar equation). DSC was applied to assess the melting point diagram of the binary mixture of crystalline NAP and γ -IND. The melting temperatures were plotted against the mole fractions of the two drugs, and the resulting phase diagram was compared to the theoretical liquidus curve predicted from the simplified form of the Schröder–Van Laar equation:¹⁵

$$\ln x = \frac{\Delta H_0}{R} \left(\frac{1}{T_0} - \frac{1}{T} \right) \quad (3)$$

where x is the mole fraction of one drug in the mixture, ΔH_0 and T_0 are the corresponding heat of fusion (J mol^{−1}) and melting temperature (K) of the pure drug substance, respectively, T is the melting point of the binary mixture at x , and R is the gas constant (8.314 J K^{−1} mol^{−1}).

3. RESULTS

3.1. Solid State Characterization. In order to investigate miscibility of the two drugs in their molten state, a phase diagram was established from the thermograms obtained by DSC. The

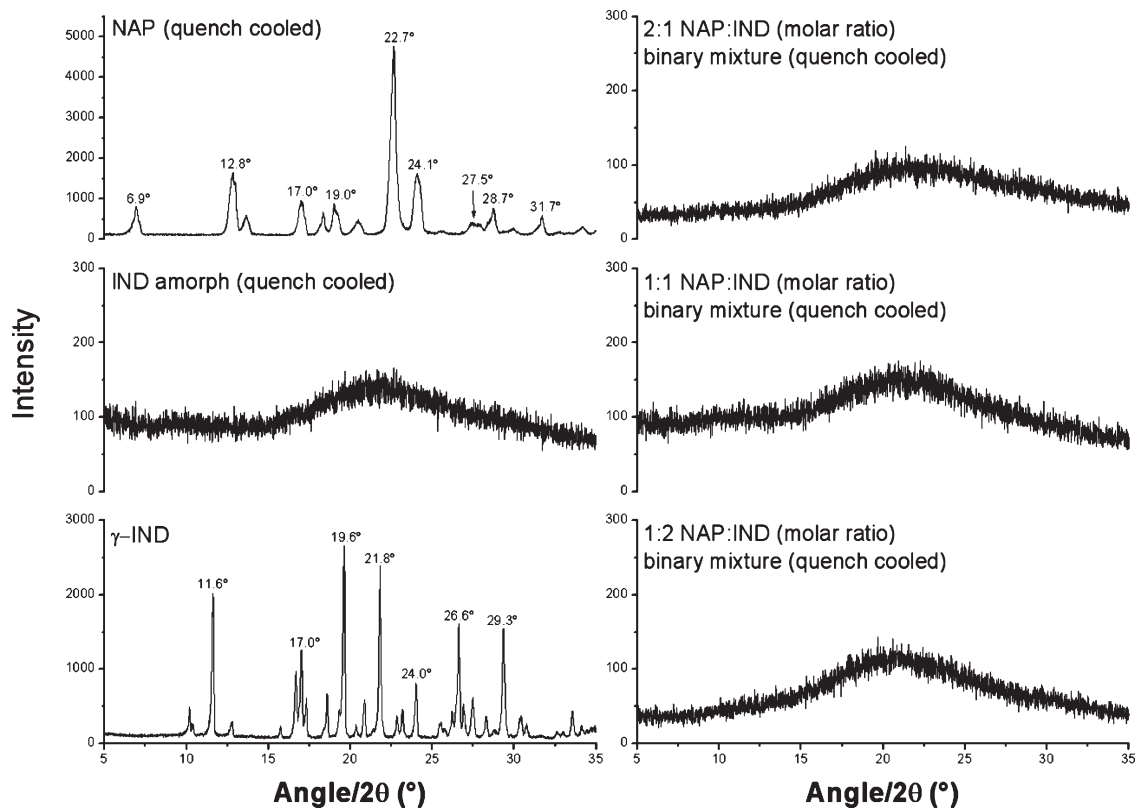


Figure 3. X-ray powder diffractograms of quench cooled NAP, quench cooled IND, γ -IND and the quench cooled mixtures of both drugs in the molar ratios 2:1, 1:1 and 1:2 (NAP:IND).

recorded data in Figure 2 shows the typical shape associated with a eutectic binary mixture. The experimental values are in good agreement with those calculated from eq 3. The 1:1 molar ratio (NAP mole fraction 0.5) is very close to the theoretical eutectic mixture (NAP mole fraction 0.55). Hence, only a single melting event at 403.85 and 404.65 K, respectively, could be detected for both mixtures in the applied experimental setup. The diagram reveals that both drugs are miscible in the liquid state. Above the liquidus curve both compounds are in their molten state and form a one phase system.¹⁵

Figure 3 shows the XRPD patterns of the freshly prepared quench cooled single drugs and the mixtures in the molar ratios 2:1, 1:1 and 1:2 (NAP:IND) as well as of crystalline γ -IND. The pattern for the quench cooled NAP shows peaks in the diffractogram and thus is a crystalline form of NAP. Peak positions of all peaks in the diffractograms were similar to the starting crystalline form, suggesting that it is in the same solid state form (data not shown). In the study, it was found that NAP in general is not easy to convert to and keep in its amorphous form due to its very high recrystallization tendency. For the other quench cooled samples, the XRPD patterns show the typical halo suggesting amorphousness.

This finding was further supported by DSC measurements, revealing a single T_g for all coamorphous drug mixtures (Figure 4, Table 1). For the single drugs, T_g s of 278.19 ± 0.37 K and 317.88 ± 0.32 K were determined for NAP and IND, respectively.

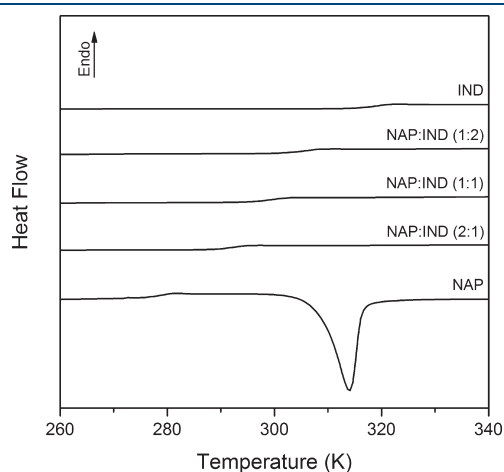


Figure 4. DSC thermograms showing the T_g s of *in situ* prepared quench cooled NAP, quench cooled IND and the quench cooled mixtures of both drugs in the molar ratios 2:1, 1:1 and 1:2 (NAP:IND).

The appearance of a single T_g for coamorphous drug mixtures indicates the formation of a homogeneous phase where one compound is dissolved in the other.¹⁶ Compounds that are not miscible (or only partially miscible) in an amorphous mixture would show two separate T_g s, one for each compound, or one T_g for a compound A- and one for a compound B-rich phase.¹⁷ The T_g s of the three mixtures are $292.04 \text{ K} \pm 0.36 \text{ K}$ (2:1 NAP:IND), $298.45 \text{ K} \pm 0.24 \text{ K}$ (1:1 NAP:IND) and $305.16 \text{ K} \pm 0.22 \text{ K}$ (1:2 NAP:IND), respectively, i.e. between those for the individual drugs.

Table 1 also shows the predicted T_g s calculated from the Gordon–Taylor equation. Initially the prediction was conducted with NAP and IND being the two compounds in the equation (i.e., no interaction between the components was assumed). It was found that all experimental values have a negative deviation from those predicted, with the 1:1 molar ratio having the highest deviation (-2.63 K). However, from the ATR-FTIR measurements intermolecular hydrogen bonding between NAP and IND in the 1:1 molar ratio was postulated (see below) and it was assumed that these interactions might play a role in the deviation from the calculated values. Taking into account the behavior of the 1:1 molar ratio samples in the stability and the intrinsic dissolution studies (see below), together with the finding that the strongest deviation of predicted from the experimental T_g was found for the 1:1 molar ratio sample (assuming no interactions), a novel approach to predict the T_g s was applied. It was assumed that both drugs at the 1:1 molar ratio may be regarded as an interconnected state, forming a heterodimer, and thus could be treated in the Gordon–Taylor equation as an individual component, with the excess drug representing the second compound. The predicted T_g s using this approach showed significantly lower deviations from the experimental values (Table 1, interactions assumed). To further test this assumption, other drug–drug mixtures with different molar ratios were prepared and analyzed for their T_g . Figure 5 shows that all predictions are in close agreement with the experimental results when calculated with the coamorphous mixture in the 1:1 molar ratio representing an individual compound in the Gordon–Taylor equation (interactions assumed).

3.2. Stability Study. The three coamorphous drug samples (ratios 2:1, 1:1 and 1:2) were stored for 21 days under dry conditions at 277.15 and 298.15 K. Figure 6 shows the obtained XRPD patterns. Interestingly the 1:1 mixture stayed amorphous over the period of storage, indicated by the appearance of a halo in the XRPD diffractograms, even though it does not have the highest T_g . In contrast, the mixtures with an excess amount of drug showed recrystallization. In the diffractograms of the 2:1 (NAP:IND) mixture distinctive peaks belonging to crystalline

Table 1. Experimental T_g s [with Standard Deviation (SD) in Parentheses] of the Pure Drugs and the Binary Mixtures at Molar Ratios 1:1, 1:2 and 2:1^a

naproxen (molar ratio)	indomethacin (molar ratio)	T_g exptl (K) (SD)	T_g predicted ^b	
			no interaction assumed	interaction assumed
pure drug		278.19 (± 0.37)		
2	1	292.04 (± 0.36)	293.75 (-1.71)	292.41 (-0.38)
1	1	298.45 (± 0.24)	300.54 (-2.10)	
1	2	305.16 (± 0.22)	306.79 (-1.63)	305.32 (-0.15)
	pure drug	317.88 (± 0.32)		

^aThe corresponding predicted T_g s are also shown. Deviations from the experimental T_g are given in parentheses. ^bGordon–Taylor equation.

NAP appear (Figures 3 and 6) for both storage temperatures, whereas the 1:2 (NAP:IND) mixture shows recrystallization of γ -IND only in the samples stored at 298.15 K (Figures 3 and 5). This behavior indicates that the T_g is not the only factor influencing stability of amorphous systems and that intermolecular interactions have to be considered (see below).

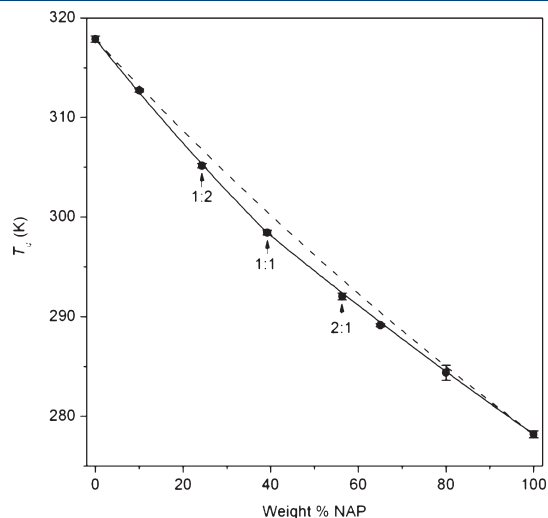


Figure 5. T_g s of coamorphous binary drug–drug mixtures of NAP and IND. The symbols represent the experimentally determined T_g values (with standard deviation), the dashed line represents the prediction of the Gordon–Taylor equation calculated from the T_g s of the single drugs (no interaction assumed), and the solid line represents the prediction with the 1:1 molar ratio sample being a separate component in the Gordon–Taylor equation next to the excess amount of drug (interaction assumed).

Based on the findings in the stability study, the 1:1 coamorphous binary combination was further analyzed and compared to the individual crystalline and amorphous drugs.

3.3. Characterization at the Molecular Level. ATR-FTIR measurements were carried out to determine possible interactions, e.g. hydrogen bonding, between both drugs. The carbonyl groups in both drugs are the most likely functional group to participate in H-bonding between the drugs, and thus, the carbonyl stretching region was selected for a detailed analysis. Figure 7 shows the collected spectra in the region from 1600 to 1800 cm^{-1} for the crystalline and amorphous individual drugs as well as their coamorphous 1:1 molar ratio sample. The spectra were normalized prior to analysis for a better visualization. For clarification of the band assignment of the two compounds, the structure formulas can be seen in Figure 8.

Crystalline NAP shows the characteristic absorption peaks at 1681 and 1725 cm^{-1} , which are assigned to the carbonyl stretch $\nu_{\text{C=O}}$ of the carboxylic acid group, where the former wavenumber represents the hydrogen-bonded carbonyl group and the latter the free carbonyl group.¹⁸ The crystalline arrangement of the NAP molecules is catamERIC, which means the carboxylic acids are hydrogen-bonded in a chainlike manner.¹⁹ Thus, there exist hydrogen-bonded and free carbonyl groups. On the other hand, the carboxylic acid groups in γ -indomethacin form a dimer structure.²⁰ Therefore, only one peak appears for the carboxylic acid in its ATR-FTIR spectrum at 1714 cm^{-1} . The peak at 1689 cm^{-1} is attributed to the second carbonyl group in the molecule, the benzoyl $\nu_{\text{C=O}}$.²¹

When substances are transformed into their amorphous counterparts, the molecular arrangement changes and the resulting IR spectra are slightly altered. Usually peaks are broader and less sharp than their crystalline analogues.²² Further, due to a different chemical environment, or rather different molecular

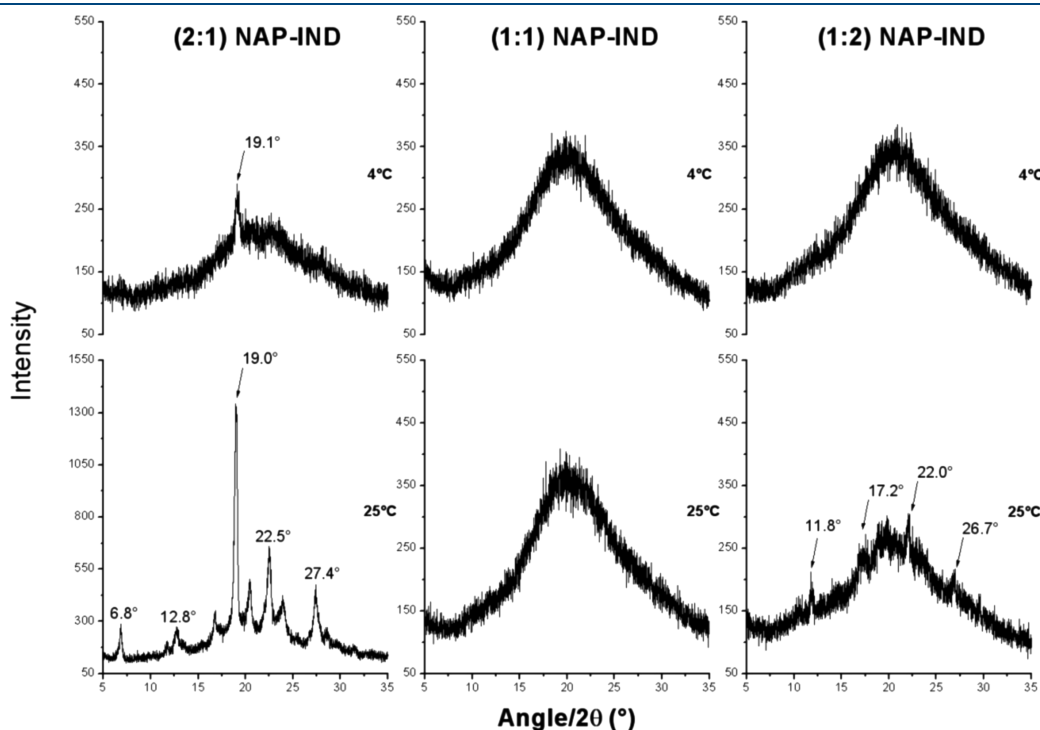


Figure 6. X-ray powder diffractograms of quench cooled coamorphous NAP-IND mixtures stored for 21 days at 277.15 and 298.15 K under dry conditions (phosphorus pentoxide). The peaks observed for the 2:1 and 1:2 sample are all related to recrystallization of the excess amount of naproxen and indomethacin, respectively.

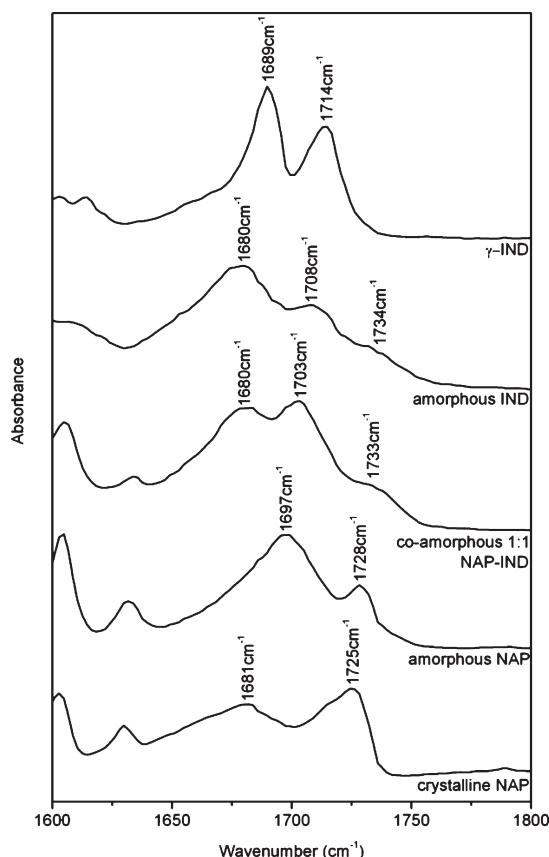


Figure 7. ATR-FTIR spectra (bottom to top) of crystalline NAP, amorphous NAP, coamorphous (1:1) NAP-IND, amorphous IND and crystalline γ -IND.

packing, peak shifts are also likely to be detected.²³ This could also be shown for the two drugs in this study. Amorphous IND shows slight shifts for the benzoyl C=O and the acid C=O to 1680 and 1708 cm^{-1} , respectively. Additionally, a shoulder at 1734 cm^{-1} appears, indicating the presence of a non-hydrogen-bonded acidic carbonyl group.²¹ IND in its amorphous form is still thought to largely form dimer structures, but at least a fraction of the molecules are not included in dimerization and, therefore, have a free carbonyl group which can be detected by FTIR.^{20,21} For amorphous NAP, shifting of peaks was also observed. The catameric carbonyl stretching peak shifts by 16 wavenumbers up to 1697 cm^{-1} and the free acid peak shifts to 1728 cm^{-1} . The large shift of the former band suggests that the molecule might undergo a rearrangement in its molecular near order. In fact the shape of the peaks is rather similar to that of the acid group in amorphous IND, pointing toward a change from the chainlike structure to possibly a dimer formation (hydrogen-bonded C=O at 1697 cm^{-1}). Analogous to the IND shoulder at 1734 cm^{-1} , a fraction of the carbonyl group in amorphous NAP is nondimerized and thus a free acid non-hydrogen-bonded carbonyl mode ($\nu_{\text{C=O}} = 1728 \text{ cm}^{-1}$) appears in the spectrum. Gupta et al. also suggested a dimerlike structure for amorphous NAP.²⁴ However, these authors also assumed a dimer structure of NAP in its crystalline state, which is not accurate according to previous publications^{19,25} and the crystal structure in the Cambridge Structural Database (CSD, Cambridge, U.K.; refcode COYRUD). Taken together, the changes observed in the spectra for the amorphous individual drugs compared to their crystalline

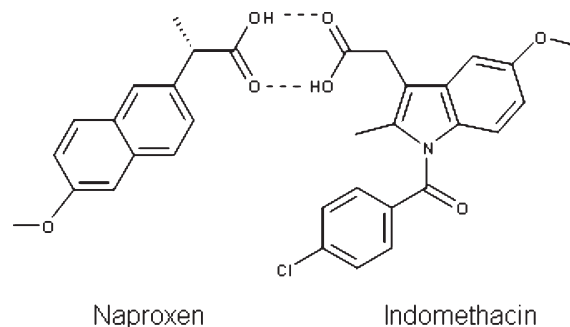


Figure 8. Chemical structures of NAP and IND. The dashed lines between the carboxylic acid groups of both drugs indicate the assumed H-bonding in the coamorphous 1:1 molar mixture.

counterparts indicate that NAP and IND form dimers in their amorphous form.

For the spectral interpretation of the 1:1 molar ratio coamorphous drug combination it is important to compare the spectra with those of the individual amorphous drugs in order to detect any interactions and differences in the spectra that are not part of changes in the solid state (crystalline to amorphous) of the individual drugs. Thus, the individual spectra of the amorphous forms of the drugs were chosen for comparison. The spectrum of the coamorphous drug combinations reveals two distinctive peaks at 1680 cm^{-1} and 1703 cm^{-1} with a very small shoulder at 1733 cm^{-1} . The shoulder can be attributed to free carboxylic acid $\nu_{\text{C=O}}$ that is also present in the amorphous individual compounds. The peak at 1703 cm^{-1} is likely to show an interaction between both acid carbonyl groups of the drugs. The intensity of the peak is increased and the hydrogen-bonded carbonyl stretchings are shifted compared to the individual drug spectra to form a new peak at an intermediate wavenumber (a downward shift of 5 cm^{-1} for $\nu_{\text{C=O}}(\text{IND}_{\text{amorph}})$ and an upward shift of 6 cm^{-1} for $\nu_{\text{C=O}}(\text{NAP}_{\text{amorph}})$ were detected). If both drugs were not interacting on the molecular level, no peak shifts should be detected for the corresponding peaks. Therefore, it is suggested that both drugs are interacting via H-bonding between their carboxylic acid groups, and we assume the formation of a hetero dimer in the coamorphous mixture similar to a hetero dimer formation in cocrystals (Figure 8). The peak position of the benzoyl C=O stretching mode of IND is the same for the coamorphous mixture and for pure amorphous IND, suggesting that this group is not involved in any H-bonding interaction.

3.4. Intrinsic Dissolution Testing. The release profiles of the two drugs in the coamorphous sample compared to their crystalline counterparts and the amorphous forms of IND are shown in Figure 9. Crystalline NAP and γ -IND have intrinsic dissolution rates (IDRs) of 0.300 ± 0.001 and $0.055 \pm 0.002 \text{ mg cm}^{-2} \text{ min}^{-1}$, respectively. These values are in good agreement with IDRs published in the literature for NAP¹² and IND.²⁶

Amorphous IND shows a significant increase over γ -IND in its IDR ($0.361 \pm 0.003 \text{ mg cm}^{-2} \text{ min}^{-1}$), and a further increase in the IDR to $0.419 \pm 0.012 \text{ mg cm}^{-2} \text{ min}^{-1}$ was determined for its coamorphous form. The IDR for NAP in the coamorphous mixture increased up to $0.411 \pm 0.003 \text{ mg cm}^{-2} \text{ min}^{-1}$.

Interestingly, the coamorphous system releases both drugs in a synchronized fashion (Figure 10). With every molecule of NAP one molecule of IND is dissolved into the dissolution medium. A similar observation was made by Allesø et al.¹² in their study on the coamorphous mixture of NAP and cimetidine.

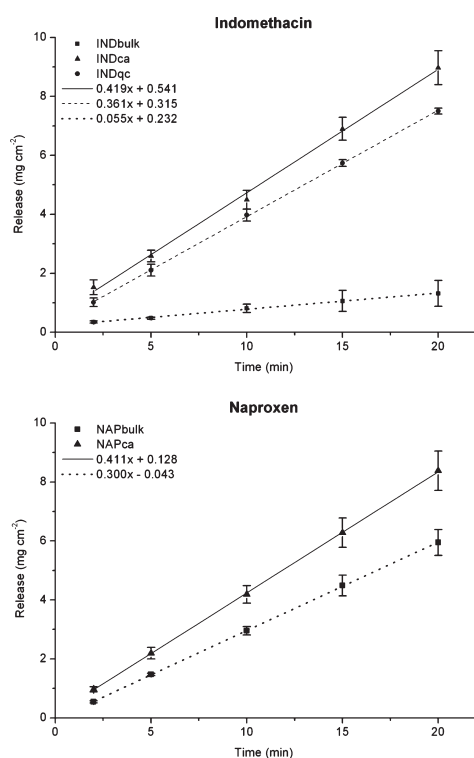


Figure 9. Intrinsic dissolution rate (IDR, $\text{mg cm}^{-2} \text{min}^{-1}$) for NAP and IND from the single crystalline and amorphous (IND) components and the quench cooled coamorphous mixture at pH 7.4, 310.15 K and 50 rpm.

4. DISCUSSION

In the drug mixtures, both drugs could be made amorphous, whereas amorphous NAP by itself is highly unstable and recrystallizes within a short time. The peak shifts in the FTIR spectra suggest that both drugs interact on the molecular level in the coamorphous form. The assumption that NAP and IND are forming a heterodimer is likely to be responsible for the behavior of the coamorphous 1:1 molar combination. This explains that the excess component is recrystallizing in the stability study for the 1:2 and 2:1 (NAP:IND) mixtures, whereas the coamorphous 1:1 combination stays in its amorphous state, even if the T_g is lower than that obtained for the 1:2 (NAP:IND) mixture. In order to recrystallize, the molecules have to break the hydrogen bonds within the heterodimer and then rearrange to form new hydrogen bonds with like molecules. Therefore, the coamorphous 1:1 mixture possesses an intrinsic resistance toward crystallization as this requires topological changes in the amorphous network. Subsequent to breaking the heterodimer hydrogen bonding, two IND molecules have to form a homodimer and naproxen molecules need to form the chainlike structure in order to recrystallize. A similar explanation is also mentioned in literature for topologically disordered amorphous compounds.²⁷ In the 1:2 and 2:1 quench cooled mixtures, the molecular short-range order for the excess amount of drug is already present and, therefore, they are readily able to recrystallize into their corresponding individual crystals.

Additionally the drug release profile of the coamorphous form further supports the assumption of a molecular interaction. The drugs dissolved in a synchronized manner due to the short-range order of the molecules (heterodimer) in the coamorphous mixture. In this regard one might hypothesize that in fact the

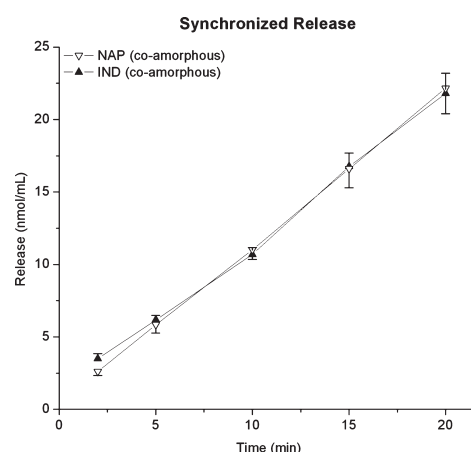


Figure 10. IDR ($\text{nmol mL}^{-1} \text{min}^{-1}$) of the coamorphous NAP-IND binary mixture demonstrates a synchronized drug release.

heterodimer is released instead of two individual amorphous drugs. Also, an increased release compared to the crystalline counterparts and amorphous indomethacin alone could be detected. This is of importance as both compounds are BCS class II drugs and the rate limiting step for absorption is their dissolution. In the case of the release of the two drugs as a heterodimer, it might be possible to further increase the dissolution rate when creating a coamorphous mixture of a BCS class II drug with a highly soluble partner to form a coamorphous mixture. Such an example was demonstrated by Allesø et al. when comilling NAP with the BCS class I drug cimetidine.¹² In this coamorphous binary mixture both drugs were also released in a synchronized manner, giving NAP a release rate of $1.49 \text{ mg cm}^{-2} \text{min}^{-1}$ compared to the $0.411 \text{ mg cm}^{-2} \text{min}^{-1}$ in this study.

In order to interpret the T_g of the various mixtures, the experimental values were compared to those predicted from the Gordon–Taylor equation. This estimation is based on the ideal free volume additivity of the individual amorphous compounds in a blend.²⁸ A negative deviation of the experimental from the predicted T_g s was found throughout all analyzed samples. Similar findings for nonideal mixing behavior in binary blends of sugars with polymers are also mentioned in literature.^{29,30} In these studies, the deviation was explained by an overall loss in the number and strength of hydrogen bonding upon mixing. Furthermore, an increase in free volume due to mixing is also a reasonable explanation for a lower than expected T_g .³⁰ In contrast, for a positive deviation of the experimentally determined T_g from the predicted value, the opposite scenario has been proposed, where the sum and strength of hydrogen bonding in the blend are higher compared to the individual amorphous compounds.^{12,31}

From the results in this study, it is suggested that the drug pair forms a heterodimer in its coamorphous state. We assume that the resulting intermolecular H-bonding plays a role in the observed T_g deviation. However, since the total number of hydrogen bonds should be equal or fairly similar to that in the individual amorphous drugs, and since both molecules possess the same functional group (i.e., carboxylic acid), involved in such a dimerization, the strength of the hydrogen bonding between like (homodimer) and unlike (heterodimer) molecules might be reasonably comparable. Therefore, an increase in free volume due to the formation of the heterodimer would explain the

deviations in the experimentally found T_g s from their prediction. When dividing the density of the amorphous phase by the density of its crystalline counterpart, one can calculate the increase in free volume. For the coamorphous 1:1 ratio mixtures this results in a 1.045-fold increase in free volume. In contrast, amorphous IND has a slightly lower increase by 1.034-fold compared to γ -IND. The density of the crystalline counterpart of the coamorphous system is 1.334 g/cm³, which is equal to the sum of the individual crystalline densities of NAP and IND. This approach implies that the 1:1 coamorphous blend exhibits a greater free volume than amorphous IND. Unfortunately, this calculation could not be carried out for NAP since its amorphous density could not be determined.

The interacting nature of both molecules in the 1:1 coamorphous mixture led to a different attempt in predicting the T_g of the mixture using the Gordon–Taylor equation. The heterodimer can be regarded as an independent compound in these mixtures for the prediction via the Gordon–Taylor equation with the excess drug representing the second component. This approach led to predicted values very close to the experimental ones. This optimized fit to the Gordon–Taylor equation suggests that excess drug and coamorphous 1:1 phase show ideal free volume additivity.

The preparation method used in this study was quench cooling. This method to obtain amorphous compounds can be of advantage, as it is a fast and solvent free process. The eutectic behavior of the two drugs may be regarded as a further advantage for the preparation of a coamorphous binary phase, as the formation of a eutectic lowers the temperature required to melt and mix the drugs. Thus, chemical degradation is reduced compared to higher temperatures needed when melting the pure drugs.³² In addition, with the possibility of applying melt extrusion as the preparative method, an efficient high throughput production method is available to produce quench cooled mixtures.³³

5. CONCLUSION

In conclusion, this study showed that coamorphous binary mixtures of small molecules are a potential strategy to improve the dissolution behavior of drugs and to stabilize the amorphous state. Quench cooling was successfully applied to obtain a homogeneous coamorphous phase. Molecular interactions could be identified with FTIR spectroscopy, and the formation of a heterodimer is suggested to explain the synchronized intrinsic dissolution as well as the higher stability of mixtures at the 1:1 molar ratio compared to mixtures at the 2:1 and 1:2 molar ratio. A novel approach to interpret deviations of experimental T_g s from the predicted ones was introduced, using the 1:1 coamorphous mixture as an individual component to be inserted into the Gordon–Taylor equation. This approach resulted in a good fit to the experimentally determined T_g s.

AUTHOR INFORMATION

Corresponding Author

*School of Pharmacy, University of Otago, P.O. Box 913, Dunedin 9054, New Zealand. Tel: +64 3 479 5410. Fax: +64 3 479 7034. E-mail: thomas.rades@otago.ac.nz.

ACKNOWLEDGMENT

The authors would like to thank Mr. Damian Walls (Dept. of Geology, University of Otago) for his help in conducting

the XRPD measurements. The Academy of Finland, Magnus Ehrnrooth Foundation and Saastamoinen Foundation are also acknowledged for funding (R.L.).

REFERENCES

- (1) Aaltonen, J.; Rades, T. Towards Physico-Relevant Dissolution Testing: The Importance of Solid-State Analysis in Dissolution. *Dissolution Technol.* **2009**, *16*, 47–54.
- (2) Hancock, B. C.; Zografi, G. Characteristics and significance of the amorphous state in pharmaceutical systems. *J. Pharm. Sci.* **1997**, *86* (1), 1–12.
- (3) Hancock, B. C.; Parks, M. What is the True Solubility Advantage for Amorphous Pharmaceuticals? *Pharm. Res.* **2000**, *17* (4), 397–404.
- (4) Kaushal, A. M.; Gupta, P.; Bansal, A. K. Amorphous drug delivery systems: Molecular aspects, design and performance. *Crit. Rev. Ther. Drug Carrier Syst.* **2004**, *21*, 133–193.
- (5) Van den Mooter, G.; Wuyts, M.; Bleton, N.; Busson, R.; Grobet, P.; Augustijns, P.; Kinget, R. Physical stabilisation of amorphous ketoconazole in solid dispersions with polyvinylpyrrolidone K25. *Eur. J. Pharm. Sci.* **2001**, *12* (3), 261–269.
- (6) Forster, A.; Hempenstall, J.; Rades, T. Characterization of glass solutions of poorly water-soluble drugs produced by melt extrusion with hydrophilic amorphous polymers. *J. Pharm. Pharmacol.* **2001**, *53* (3), 303–315.
- (7) Vasconcelos, T.; Sarmento, B.; Costa, P. Solid dispersions as strategy to improve oral bioavailability of poor water soluble drugs. *Drug Discovery Today* **2007**, *12* (23–24), 1068–1075.
- (8) Serajuddin, A. T. M. Solid dispersion of poorly water-soluble drugs: Early promises, subsequent problems, and recent breakthroughs. *J. Pharm. Sci.* **1999**, *88* (10), 1058–1066.
- (9) Shrivastava, A. R.; Ursekar, B.; Kapadia, C. J. Design, Optimization, Preparation and Evaluation of Dispersion Granules of Valsartan and Formulation into Tablets. *Curr. Drug Delivery* **2009**, *6*, 28–37.
- (10) Kaur, R.; Grant, D. J. W.; Eaves, T. Comparison of polyethylene glycol and polyoxyethylene stearate as excipients for solid dispersion systems of griseofulvin and tolbutamide II. *J. Pharm. Sci.* **1980**, *69* (11), 1321–1326.
- (11) Chieng, N.; Aaltonen, J.; Saville, D.; Rades, T. Physical characterization and stability of amorphous indomethacin and ranitidine hydrochloride binary systems prepared by mechanical activation. *Eur. J. Pharm. Biopharm.* **2009**, *71* (1), 47–54.
- (12) Allesø, M.; Chieng, N.; Rehder, S.; Rantanen, J.; Rades, T.; Aaltonen, J. Enhanced dissolution rate and synchronized release of drugs in binary systems through formulation: Amorphous naproxen-cimetidine mixtures prepared by mechanical activation. *J. Controlled Release* **2009**, *136* (1), 45–53.
- (13) Yamamura, S.; Gotoh, H.; Sakamoto, Y.; Momose, Y. Physico-chemical properties of amorphous precipitates of cimetidine-indomethacin binary system. *Eur. J. Pharm. Biopharm.* **2000**, *49* (3), 259–265.
- (14) Yamamura, S.; Gotoh, H.; Sakamoto, Y.; Momose, Y. Physico-chemical properties of amorphous salt of cimetidine and diflunisal system. *Int. J. Pharm.* **2002**, *241* (2), 213–221.
- (15) Carstensen, J. T. *Advanced pharmaceutical solids*; Marcel Dekker: New York, 2001; Vol. 110.
- (16) Chiou, W. L.; Riegelman, S. Pharmaceutical applications of solid dispersion systems. *J. Pharm. Sci.* **1971**, *60* (9), 1281–1302.
- (17) van Drooge, D. J.; Hinrichs, W. L. J.; Visser, M. R.; Frijlink, H. W. Characterization of the molecular distribution of drugs in glassy solid dispersions at the nano-meter scale, using differential scanning calorimetry and gravimetric water vapour sorption techniques. *Int. J. Pharm.* **2006**, *310* (1–2), 220–229.
- (18) del Arco, M.; Gutiérrez, S.; Martín, C.; Rives, V.; Rocha, J. Synthesis and characterization of layered double hydroxides (LDH) intercalated with non-steroidal anti-inflammatory drugs (NSAID). *J. Solid State Chem.* **2004**, *177* (11), 3954–3962.
- (19) Ravikumar, K.; Rajan, S. S.; Pattabhi, V. Structure of Naproxen, C₁₄H₁₄O₃. *Acta Crystallogr.* **1985**, *C41*, 280–282.

- (20) Aaltonen, J.; Gordon, K. C.; Strachan, C. J.; Rades, T. Perspectives in the use of spectroscopy to characterise pharmaceutical solids. *Int. J. Pharm.* **2008**, *364* (2), 159–169.
- (21) Taylor, L. S.; Zografi, G. Spectroscopic Characterization of Interactions Between PVP and Indomethacin in Amorphous Molecular Dispersions. *Pharm. Res.* **1997**, *14* (12), 1691–1698.
- (22) Heinz, A.; Gordon, K. C.; McGoverin, C. M.; Rades, T.; Strachan, C. J. Understanding the solid-state forms of fenofibrate - A spectroscopic and computational study. *Eur. J. Pharm. Biopharm.* **2009**, *71* (1), 100–108.
- (23) Strachan, C. J.; Rades, T.; Gordon, K. C. A theoretical and spectroscopic study of γ -crystalline and amorphous indometacin. *J. Pharm. Pharmacol.* **2007**, *59* (2), 261–269.
- (24) Gupta, M. K.; Bogner, R. H.; Goldman, D.; Tseng, Y.-C. Mechanism for Further Enhancement in Drug Dissolution from Solid-Dispersion Granules upon Storage. *Pharm. Dev. Technol.* **2002**, *7* (1), 103–112.
- (25) Kim, Y.; Song, H.; Park, I. Refinement of the structure of naproxen, (+)-6-methoxy- α -methyl-2-naphthaleneacetic acid. *Arch. Pharmacol. Res.* **1987**, *10* (4), 232–238.
- (26) Wu, T.; Sun, Y.; Li, N.; de Villiers, M. M.; Yu, L. Inhibiting Surface Crystallization of Amorphous Indomethacin by Nanocoating. *Langmuir* **2007**, *23* (9), 5148–5153.
- (27) Gupta, P. K. Non-crystalline solids: glasses and amorphous solids. *J. Non-Cryst. Solids* **1996**, *195* (1–2), 158–164.
- (28) Shamblin, S. L.; Huang, E. Y.; Zografi, G. The effects of co-lyophilized polymeric additives on the glass transition temperature and crystallization of amorphous sucrose. *J. Therm. Anal. Calorim.* **1996**, *47* (5), 1567–1579.
- (29) Taylor, L. S.; Zografi, G. Sugar–polymer hydrogen bond interactions in lyophilized amorphous mixtures. *J. Pharm. Sci.* **1998**, *87* (12), 1615–1621.
- (30) Shamblin, S. L.; Taylor, L. S.; Zografi, G. Mixing behavior of co-lyophilized binary systems. *J. Pharm. Sci.* **1998**, *87* (6), 694–701.
- (31) Gupta, P.; Thilagavathi, R.; Chakraborti, A. K.; Bansal, A. K. Role of Molecular Interaction in Stability of Celecoxib–PVP Amorphous Systems. *Mol. Pharmaceutics* **2005**, *2* (5), 384–391.
- (32) Forster, A.; Hempenstall, J.; Tucker, I.; Rades, T. The Potential of Small-Scale Fusion Experiments and the Gordon-Taylor Equation to Predict the Suitability of Drug/Polymer Blends for Melt Extrusion. *Drug Dev. Ind. Pharm.* **2001**, *27* (6), 549–560.
- (33) Breitenbach, J. Melt extrusion: from process to drug delivery technology. *Eur. J. Pharm. Biopharm.* **2002**, *54* (2), 107–117.